Water Soluble Copolymers for Calcium Carbonate and Calcium Sulphate Scale Control in Cooling Water Systems

P. Shakkthivel, D. Ramesh, R. Sathiyamoorthi, T. Vasudevan

Department of Industrial Chemistry, Alagappa University, Karaikudi 630 003, Tamil Nadu, India

Received 3 July 2003; accepted 12 October 2004
DOI 10.1002/app.21588
Published online in Wiley InterScience (www.interscience.wiley.com).

ABSTRACT: Mineral scales are formed in cooling water systems and they cause heat transfer problems. Much research has been carried out to reduce the carbonate and sulphate scales of calcium. To inhibit the scale formation in cooling water systems, vinyl acetate–acrylic acid (VA–AA) and vinyl acetate– methacrylic acid (VA–MAA) copolymers were synthesized, characterized, and the ability of the polymers to mitigate the calcium carbonate and calcium sulphate scale formation was tested through chemical screening, constant potential electrolysis, and electrochemical impedance techniques. XRD (X-ray diffraction) and SEM (scanning electron microscope) studies were performed to understand the morphological changes of the scales in the presence of the polymers. The biocidal, gelation, and iron dispersion ability of the polymers were also noted. Among the two threshold inhibitors, VA–AA shows slightly better antiscaling properties even at higher temperatures and pH for both $CaCO_3$ and $CaSO_4$ scales compared to the methacrylic copolymer. © 2005 Wiley Periodicals, Inc. J Appl Polym Sci 96: 1451–1459, 2005

Key words: antiscalant; water-soluble polymers; scanning electron microscopy; x-ray difraction; gelation and biocidal properties

INTRODUCTION

Cooling towers and systems experience scaling on metal surfaces. The scales are formed from carbonates and sulphates of magnesium, calcium, and barium together with iron oxide, silica, and biological contaminants. Deposition of these materials on heat exchange surfaces can lead to loss of system efficiency, unscheduled shutdown, and ultimately to system failures or clogging of filters, obstruction of fluid flow, reduction in cooling efficiency, localized corrosion attack, wear of metal parts, and loss of production and economy.[1–3] The scale formation depends on concentration of lattice forming ions, dissolved and suspended solids, pH, flow velocity, evaporation rate, pressure, etc.[4,5] Scales can be controlled by (1) altering the system design and operating parameters, (2) altering the nature of feed waters, and (3) using chemical treatment methods. Naturally occurring polymers have been used for scale control but their use is restricted as they have been found to decompose at higher temperatures.[6] When chelating agents are used, they form soluble complexes with lattice forming ions. A stoichiometric amount is needed and pH range must also be precise with their use. Hence, their application is costly and limited. One of the chemical methods to control scale is the use of threshold inhibitors. Water-soluble low molecular weight homopolymers and copolymers deserve much attention in their class. The present work deals with the synthesis and application of some vinyl acetate polymers for cooling water systems.

Correspondence to: T. Vasudevan (apsakthivel@yahoo.com).

Journal of Applied Polymer Science, Vol. 96, 1451–1459 (2005)

EXPERIMENTAL PROCEDURE

Synthesis of vinyl acetates

Copolymers of vinyl acetate–acrylic acid and vinyl acetate–methacylic acid were synthesized in aqueous medium through free radical polymerization.[7,8] The polymerization was carried out in an inert atmosphere. Diluted vinyl acetate monomer was copolymerized with diluted acrylic acid and methacrylic acid with potassium peroxodisulphate as the initiator.

Characterization

The viscosity of the polymers was found with a Efflex viscometer. The synthesized copolymers were characterized through FT-IR spectra to confirm the functional groups, which are responsible for the antiscaling property of the antiscalant polymers using a Perkin-Elmer FT-IR spectrometer, PARAGON model 500.

Evaluation of antiscalants

Chemical screening test

The ability of the polymers to mitigate mineral salts precipitation such as calcium carbonate and calcium

sulphate was assessed through an EDTA titration method as per NACE standard.[9] 300 ppm of hard water was used as the test solution for the calcium carbonate scale control and different dosage levels of the polymers were added to the test solutions along with the blank solution. The tests were carried out in the temperature range 50–80°C and in the pH range 7.0–8.5. The test cells were placed in a constant temperature water bath to maintain the required temperatures for 12 h. After the test period, the cells were allowed to cool for 12 h without disturbance to settle the scale. The hardness of the test solution was then estimated by titrimetric method. The same procedure was adopted for the calcium sulphate brine, but the hardness was fixed at 2,000 ppm.

Constant potential electrolysis

Constant potential electrolysis was performed using EG & G Princeton Applied Research (PAR) VersaStat II. A three-electrode cell assembly was used with two 1×1 cm platinum foils as working and counter electrode and a saturated calomel electrode (SCE) as the reference. The tests were carried out by applying -1.2 V Vs SCE to the working electrode dipped in 300 ppm $CaCO_3$ brine with different dosage levels of the polymers. The change in current density with time was recorded.[10,11]

AC Impedance technique

EG & G PAR model 398 Electrochemical Impedance Analyzer with a three- electrode cell assembly as mentioned above was used. The $CaCO_3$ scale formation was accelerated on the platinum electrode by applying -1.2 V Vs SCE to the working electrode for 30 min. After the scaling, impedance measurements were made over a frequency range of 100 mHz–10 kHz with 5 mV ac amplitude being superimposed over the steady-state potential of the systems.[11,12] The spectra were recorded for the blank brine and the polymer-treated samples.

SEM and XRD studies

The change of crystal habits by the addition of antiscalants was examined through SEM and XRD. Gold coating was applied to the surface to make it conductive, if needed, using the JFC 100-E ion sputtering device to take SEM photographs using a JOEL JSM 840A scanning microscope. X-ray diffraction studies were also done for the scales in the presence and absence of the scale inhibitors with a JOEL-8030 X-ray diffractometer.

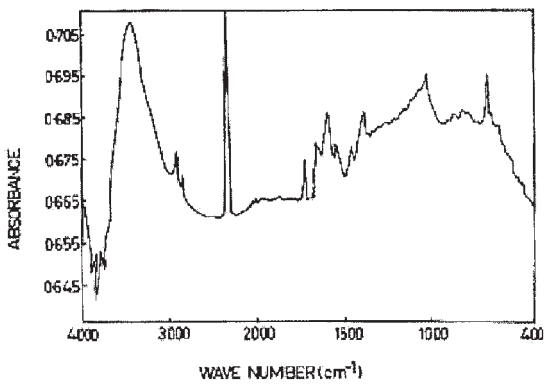

Figure 1 FT-IR spectrum of vinyl acetate–acrylic acid copolymer (VA–AA).

Iron-dispersing ability and gelation test

The iron-dispersing ability of the polymers were tested using synthetically prepared hydrated iron oxide solution using 100 mg/L iron ion and sodium bicarbonate. 20 ppm of the antiscalants was added to the test solutions and allowed to stand for 24 h at 50°C and pH 8.5. After the above period, the iron hydroxide [$Fe(OH)_3$] was centrifuged and the supernatant solutions were analyzed for iron ion retained in the solutions using an UV-visible spectrometer.[13,14]

The calcium–polymer bridging was tested using 20 ppm of the polymer dosage added to 300 ppm of calcium ion solution. The test solutions were buffered by adding 2 ml of borate buffer and the pH was adjusted to 8.5, stirred for 1 h at 50°C. The absorbency of the test solutions were measured by a UV-visible spectrometer.[14]

Biocidal properties

The algae- and microorganism-killing properties of the polymer were tested through a $\times 45$ microscope and conventional agar diffusion and serial dilution techniques, respectively. For the biocidal testing, the culture was mixed and, for the algae-killing property, water containing 14 different major algae was used.

RESULTS AND DISCUSSION

Characterization

The intrinsic viscosities of the polymers were determined using the Efflex viscometer. The viscosity for water, VA–AA, and VA–MAA was 1.0, 1.7, and 4.8, respectively. The values indicate the low molecular weight of the polymers. Figures 1 and 2 show the FTIR for the VA–AA and VA–MAA, respectively. In the case of the polymer VA–AA, the peaks at 1610 and 1552 cm^{-1} are for the asymmetric and symmetric stretching vibration of the COO^-. The peaks at 1727

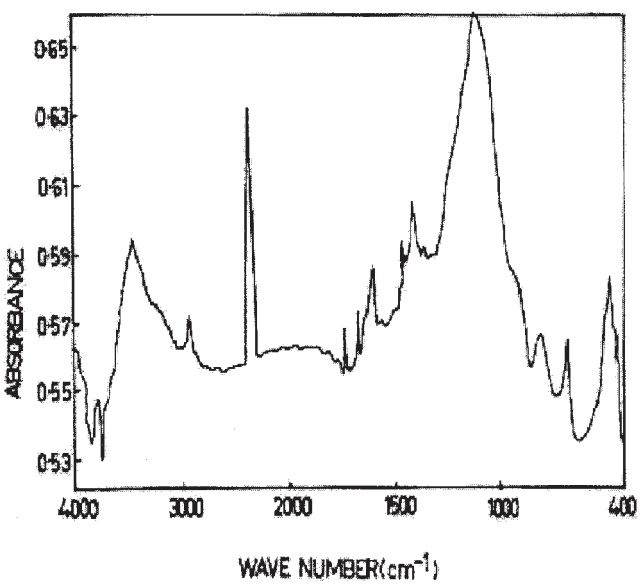

Figure 2 FT-IR spectrum of vinyl acetate–methacrylic acid copolymer (VA–MAA).

and 1663, and 1466 cm^{-1} correspond to the stretching vibration of COO^- in the ester group and the scissoring deforming vibration of the methylene group.

In Figure 2, the peak at 1662 cm^{-1} is for the COO^- stretching vibration. Due to the inductive effect of CH_3, the stretching vibration of COO^- appears at 1662 cm^{-1}. The peaks at 2950 and 1406 cm^{-1} are for the C–CH_3 band vibration and the C–CH_3 bending vibration, respectively. The COO^- stretching vibration in the ester group and the CH_2 scissoring deformation vibration peaks appear at 1725 and 1460 cm^{-1}, respectively.[15,16]

Evaluation of the antiscalant

The ability of the antiscalants in blocking the calcium carbonate scale formation was evaluated through chemical and electrochemical techniques. In the absence of any electrochemical method to accelerate the calcium sulphate scale formation, the only available chemical screening test was performed.

Chemical screening test

For the evaluation of the polymers, the solutions were prepared as per NACE standard.[9] Table I presents the results for VA–AA at 50–80°C in the pH range of 7.0–8.5 for 300 ppm $CaCO_3$ hardness brine. The antiscaling efficiency is increased with increasing polymer dosage. Except for the very slight decrease in efficiency at 70 and 80°C at pH 8.5 at the higher dosage level of 20 ppm, 100% efficiency was noted. Table II shows the results for the VA–MAA polymer on the $CaCO_3$ scale mitigation. With 20 ppm dosage, 100%

TABLE I
Antiscaling Efficiency of VA–AA Copolymer on Calcium Carbonate Scale (300 ppm as Calcium Hardness) at Different Temperatures and pHs Through Chemical Screening Test

Sl. No.	Temperature (°C)	Dosage level (ppm)	Percentage efficiency			
			pH 7.0	pH 7.5	pH 8.0	pH 8.5
1		Blank	—	—	—	—
2		1	45	51	42	38
3	50	2	63	59	57	52
4		5	80	78	72	67
5		10	100	100	95	93
6		20	100	100	100	100
1		Blank	—	—	—	—
2		1	61	56	48	43
3	60	2	69	63	55	51
4		5	78	74	81	76
5		10	100	100	91	87
6		20	100	100	100	100
1		Blank	—	—	—	—
2		1	57	49	46	41
3		2	64	58	50	50
4	70	5	73	70	78	71
5		10	100	97	89	85
6		20	10	100	100	98
1		Blank	—	—	—	—
2		1	51	42	41	33
3		2	58	54	50	46
4	80	5	69	68	71	66
5		10	98	92	86	83
6		20	100	100	99	94

TABLE II
Antiscaling Efficiency of VA–MAA Copolymer on Calcium Carbonate Scale (300 ppm as Calcium Hardness) at Different Temperatures and pHs Through Chemical Screening Test

Sl. No.	Temperature (°C)	Dosage level (ppm)	Percentage efficiency			
			pH 7.0	pH 7.5	pH 8.0	pH 8.5
1		Blank	—	—	—	—
2		1	43	40	38	36
3	50	2	55	53	49	48
4		5	91	87	85	82
5		10	98	95	95	90
6		20	100	100	98	95
1		Blank	—	—	—	—
2		1	40	39	35	33
3	60	2	53	50	48	45
4		5	90	86	83	80
5		10	95	94	91	87
6		20	97	97	93	90
1		Blank	—	—	—	—
2		1	40	37	35	31
3		2	50	50	49	47
4	70	5	89	87	81	78
5		10	93	90	89	85
6		20	97	92	90	86
1		Blank	—	—	—	—
2		1	38	37	32	30
3		2	50	45	43	35
4	80	5	85	84	81	81
5		10	90	88	85	80
6		20	95	91	89	81

efficiency is present only up to pH 7.5 at 50°C; at higher temperatures and pHs, the efficiency falls to nearly 80%.

The inhibition efficiency of the VA–AA and VA–MAA on calcium sulphate scale inhibition are presented in Tables III and IV, respectively. In the case of VA–AA polymer, with 10 ppm concentration, for all the pHs at 50°C, there is 100% efficiency and also 100% efficiency was noted at temperatures up to 7.5 pH. At higher pHs and temperatures, the efficiency decreases. With the 20 ppm dosage, there is 100% efficiency at all pHs and temperatures except at the highest pH (8.5) and temperature (80°C), where the efficiency is 97%. In the case of VA–MAA polymer with the 10 ppm dosage, a maximum efficiency of 95% was obtained at pH 7.0 and 50°C. With increase in pH and temperature, the efficiency is reduced. At the 20 ppm dosage with higher temperatures, pH, the efficiency is lowered to 94%.

Constant potential electrolysis

The scaling of $CaCO_3$ was accelerated on a platinum electrode at a potential at which the electrochemical reduction of the dissolved oxygen in the test brine is realized. The current–time curve is obtained by applying −1.2 V Vs SCE to the working electrode for 30 min in 300 ppm of hard water brine.

The pH is controlled by the carbon dioxide equilibrium in water,

$$CO_2 + H_2O \rightarrow H_2CO_3 \quad (1)$$

$$H_2CO_3 \rightarrow H^+ + HCO_3^- \quad (2)$$

$$HCO_3^- \rightarrow H^+ + CO_3^{2-} \quad (3)$$

The OH^- ions on the metal electrode in neutral medium are produced

$$H_2O + 1/2O_2 + 2e^- \leftrightarrow 2OH^- \quad (4)$$

in a few cases:

$$2H_2O + 2e^- \leftrightarrow H_2 + 2OH^- \quad (5)$$

the production of OH^- ions enhances the buffering reaction in solution:

$$OH^- + HCO_3^- \leftrightarrow H_2O + CO_3^{2-} \quad (6)$$

$$CO_3^{2-}Ca^{2+} \rightarrow CaCO_3(ppt) \quad (7)$$

The higher concentration of CO_3^{2-} ions increases the precipitation of $CaCO_3$. The current–time curve pre-

TABLE III
Antiscaling Efficiency of VA–AA Copolymer on Calcium Sulphate Scale (2,000 ppm as Calcium Hardness) at Different Temperatures and pHs Through Chemical Screening Test

Sl. No.	Temperature (°C)	Dosage level (ppm)	Percentage efficiency			
			pH 7.0	pH 7.5	pH 8.0	pH 8.5
1		Blank	—	—	—	—
2		1	55	53	49	45
3	50	2	72	70	63	63
4		5	97	90	86	85
5		10	100	100	100	98
6		20	100	100	100	100
1		Blank	—	—	—	—
2		1	56	55	48	45
3	60	2	71	68	69	65
4		5	97	92	85	79
5		10	100	100	89	96
6		20	100	100	100	100
1		Blank	—	—	—	—
2		1	53	50	47	46
3		2	70	67	67	60
4	70	5	94	90	83	78
5		10	100	100	98	93
6		20	100	100	100	100
1		Blank	—	—	—	—
2		1	52	50	45	43
3		2	72	68	65	60
4	80	5	91	85	79	74
5		10	100	99	92	79
6		20	100	100	100	97

TABLE IV
Antiscaling Efficiency of VA–MAA Copolymer on Calcium Sulphate Scale (2,000 ppm as Calcium Hardness) at Different Temperatures and pHs Through Chemical Screening Test

Sl. No.	Temperature (°C)	Dosage level (ppm)	Percentage efficiency			
			pH 7.0	pH 7.5	pH 8.0	pH 8.5
1		Blank	—	—	—	—
2		1	40	38	35	35
3	50	2	50	50	47	46
4		5	70	68	65	60
5		10	95	91	86	81
6		20	100	100	100	95
1		Blank	—	—	—	—
2		1	39	38	36	34
3	60	2	48	45	44	42
4		5	70	66	62	60
5		10	91	88	85	81
6		20	100	100	98	95
1		Blank	—	—	—	—
2		1	34	32	33	30
3		2	45	42	40	39
4	70	5	68	65	64	56
5		10	89	85	80	73
6		20	100	100	95	89
1		Blank	—	—	—	—
2		1	33	31	29	27
3		2	42	42	40	39
4	80	5	85	84	83	52
5		10	92	90	79	68
6		20	100	100	94	77

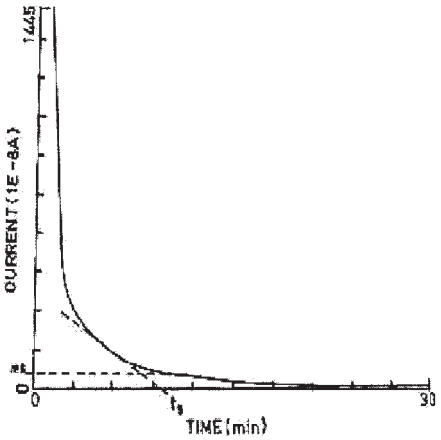

Figure 3 Characteristic current–time curve obtained through constant potential electrolysis of hard water containing 300 ppm of Ca^{2+}.

sented in Figure 3 consists of two distinct portions. The calcareous deposits, isolate the metal from the solution and consequently the rate of O_2 reduction is reduced. The sudden decay part is due to the increasing coverage of the $CaCO_3$ deposit on the electrode surface. The scaling time is the time required for full coverage of scale, and the residual current is related to the morphology of the scale.[10,17,18] If the insulating layer is highly compact, the residual current is very low.

The constant potential electrolysis was carried out with 300 ppm hardness with the presence of VA–AA and VA–MAA at pH 8.0 and the results are presented in Table V. The residual current and scaling time for the control are 34.43 μA and 112 s, respectively. With the addition of the polymer, the values are increased. This indicates the retardation or modification of the calcareous deposit formation in the presence of the polymer.

Electrochemical impedance spectroscopy

The well-separated two time constant nyquist plots were recorded during the scaling process on a platinum electrode immersed in a calcium ion–containing solution.[10,17–20] In one of the electrochemical techniques, the $CaCO_3$ scale deposition was detected by the decrease of O_2 reduction limiting diffusion currents due to the coverage of scale on the electrode.

In the impedance plot, the loop at high frequency range gives the pseudo high frequency resistance (R_{HF}) and pseudo high capacitance (C_{HF}), accounting for the surface coverage and the rate of scaling on the metal surface. The loop at the low frequency region accounts for the oxygen diffusion in the bulk solution and it is usually neglected. The values of R_{HF}, C_{HF}, the blocking ratio (σ), and the coverage rate at the surface (θ) by the calcareous scale are given as

$$R_{HF} \approx R_t\left(\frac{1+\sigma_\theta}{1+\frac{R_t}{R_{t\theta}}\sigma_\theta}\right)$$

where

$$\sigma_\theta = \sigma\left(1+\frac{kI^*}{D}\right)$$

and

$$C_{HF} = \frac{C}{1+\sigma}$$

where D is the diffusion coefficient and C is the change of double layer capacity.

C_{HF} could be considered as a means to estimate directly the blocking ratio σ through the following equation:

$$\sigma = \frac{C_{HF}(\sigma = \theta) - C_{HF}}{C_{HF}}$$

and the coverage rate of the surface θ by calcereous scale, as:

$$\theta = \frac{S_2}{S_1+S_2} = \frac{\sigma}{1+\sigma}$$

where S_1 is the free surface of metal electrode and S_2 is the partially scaled area of the electrode, where θ varies from 0 to 1 and σ changes from 0 to α.

The performance of the polymer on scale inhibition is presented in Figure 4–6. The C_{dI} and R_t values are very much changed compared with those for the control. The nyquist plots were used to find the R_t values

TABLE V
Scaling Time and Residual Current for Calcium Carbonate Scaling (300 ppm of Hardness) Obtained from Constant Potential Electrolysis at pH 8.0 with Different Dosage Levels of VA–AA and VA–MAA Polymers

S. No.	Name of antiscalant	Dosage level (ppm)	Residual current (μA)	Scaling time (s)
1	VA–AA	Blank	34.43	662
2		1	40.05	690
3		2	50.20	825
4		5	51.98	841
5		10	64.89	951
6		20	150.50	1,627
1	VA–MAA	1	45.75	695
2		2	47.33	701
3		5	61.90	896
4		10	70.14	1,039
5		20	149.20	1,616

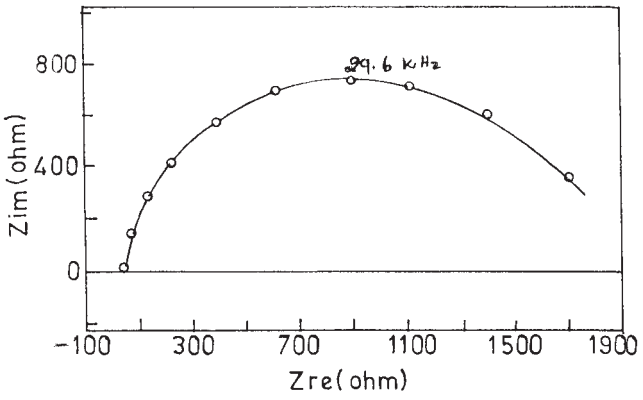

Figure 4 Nyquist plot obtained after calcium carbonate scaling on the platinum electrode immersed in calcium carbonate brine containing 300 ppm of Ca^{2+} ions.

and $2\pi F_{max}R_tC_{dI} = 1$ expression for the capacitance value. The insulating $CaCO_3$ made a definite resistance value compared to the bare metal for the O_2 reduction reaction and the capacity is related to the dielectric nature of the scales. The percentage inhibition of the scale formation was calculated from

$$\% = \frac{(R_t)_{control} - (R_t)_{inhibitor}}{(R_t)_{control}}$$

The R_t value for the control is 1680 ω/cm^2 and the C_{dl} value is 0.0032 $\mu F/cm^2$. With the addition of the polymer, the R_t and C_{dl} values are drastically changed to around 20 ω/cm^2 and 3$\mu F/cm^2$, respectively. This is due to the free oxygen reduction at the electrode surface that has become possible with the use of the antiscalants. Thus, the results reiterate the effectiveness of the polymers on the scale mitigation. This conforms to the results obtained from the constant potential electrolysis and chemical screening tests.

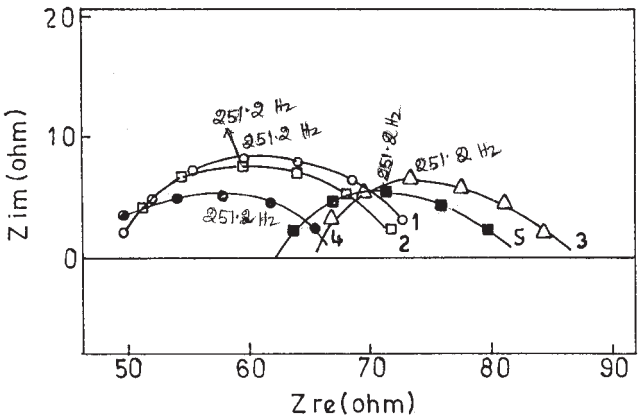

Figure 5 Electrochemical impedance spectrum for calcium carbonate scale in carbonate brine with different concentrations of VA–AA copolymer: (1) 1 ppm, (2) 2 ppm, (3) 5 ppm, (4) 10 ppm, and (5) 20 ppm.

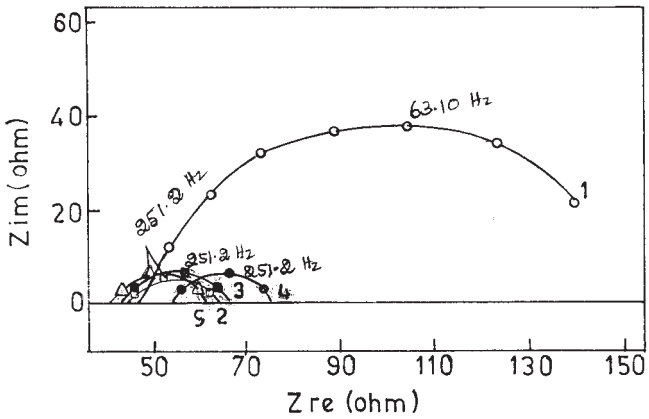

Figure 6 Electrochemical impedance spectrum for calcium carbonate scale in carbonate brine with different concentrations of VA–MAA copolymer: (1) 1 ppm, (2) 2 ppm, (3) 5 ppm, (4) 10 ppm, and (5) 20 ppm.

SEM and XRD studies

SEM is one of the widely used nondestructive surface examination techniques. The effect of antiscaling polymers on the morphology of the $CaCO_3$ and $CaSO_4$ scale was examined.

The photographs for $CaCO_3$ without and with the presence of the polymers are presented in Figure 7(a–c). The presence of Mg^{2+} ions showed the effect on the crystal morphology of $CaCO_3$ phases.[21,22] The distorted cubic structures of $CaCO_3$, calcite crystals have been identified in the present study and no effect was observed with Mg^{2+}. With the presence of the polymer, the nucleation rates are increased and the growth rates are reduced. The crystallinity of the scale is not affected much.

Figure 8(a–c) shows $CaSO_4$ scales without and with the presence of the polymers. The crystal types of $CaSO_4$ depend on the evaporation rate of water and forms, dihydrate, hemihydrate, and anhydrate. Calcium sulphate dihydrate crystals are reported as thin tubular cells and needles exhibiting monoclinic symmetry.[23] Amjad[2] has studied the effect of polyacrylate on the formation of calcium sulphate dihydrate scales and claims that the structure of the crystals are highly modified. In the present study, the crystals formed correspond to the dihydrate geometry. The change in

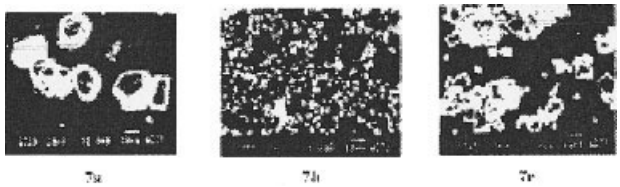

Figure 7 SEM photographs of calcium carbonate crystals at ×1000 magnification: (a) Blank; (b) with VA–AA polymer; and (c) with VA–MAA polymer.

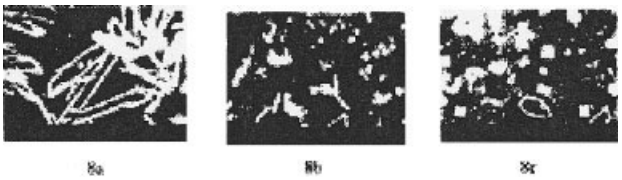

Figure 8 SEM photographs of calcium sulphate crystals at ×1000 magnification: (a) Blank; (b) with VA–AA polymer; and (c) with VA–MAA polymer.

the crystallinity and crystal habit is noted with the presence of the polymer.

The XRD results for the carbonate and sulphate crystals of calcium without and with the presence of the polymer are presented in Figures 9 (a and b) and 10 (a and b), respectively. For calcium carbonate and calcium sulphate scales, d and θ values conform to those for the calcite crystals[24] and $CaSO_4.2H_2O$ crystals.[25] In both cases, the addition of polymers did not alter the crystal structure, as confirmed by no alteration in their d and θ values. Only the crystal habit or morphology is changed, as is evident from the SEM photographs.

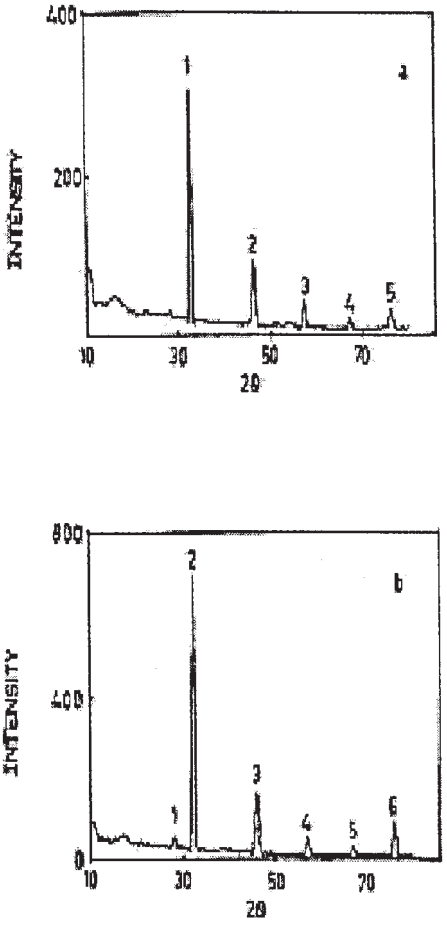

Figure 9 XRD spectrum: (a) for calcium carbonate and (b) in presence of VA–AA.

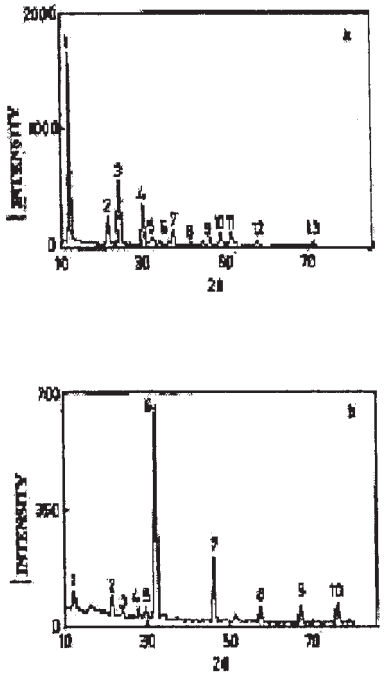

Figure 10 XRD spectrum: (a) for calcium sulphate and (b) in presence of VA–AA.

Iron dispersing and gelating ability of the polymers

Most of the cooling water pipe lines are made of iron and, in this case, Fe^{2+} ion may leach out as a corrosion product. If the antiscalant retains the Fe^{2+} ion in solution, the system can be saved from further corrosion. The complexing ability of the polymers with iron ion and with calcium ion were studied through UV-visible spectroscopy and the results show that both the polymers have the tendency to bridge with Fe^{2+} ions. The iron ion forms a complex with free carboxylate ions of the polymers in the wave length region 270–275 nm.

The appearance was noted of opalescence or turbidity when the polymeric antiscalant was added to calcium containing water, this is called gelation or calcium–polymer gel formation.[26] Among the two polymers tested, only VA–MAA showed gelation properties, through the bridging of Ca^{2+} ions with the carboxyl group resulting in slight turbid appearance was noted. Hence, the polymer requirement for water treatment may require a slightly increased dosage.

Microbiocidal property

Raw water containing various algae was used for this study. The effect of the polymer on algae was tested with 500 ppm of the antiscalants in 100 ml of the sample. After a 3-h test period, the density of algae present in the water was tested. Among 14 different major algae present in test sample, only *Anebaena*, *Ulothrix*, *Chlorella*, and *Agmenellum* are noted to be

present. The biocidal properties of the polymers were tested and showed no killing properties on noted microorganisms.

CONCLUSION

The copolymers VA–AA and VA–MAA have been synthesized and characterized through FT-IR studies. The viscosity of the polymer for VA–AA was found to be very low compared to that for VA–MAA copolymer. Still, both polymers are freely water soluble. The polymer VA–AA gives around 100% efficiency even at higher pH (8.5) and temperature (80°C) with a 20 ppm dosage. Electrochemical studies such as constant potential electrolysis and impedance measured and established their good antiscaling property. SEM and XRD studies show the crystal structures are not much altered but the antiscalants bring about changes in crystal habits or crystal morphology. The threshold scale of inhibition of the polymers is due to their adsorption on the growing crystal phases of the nuclei, which results in the distortion and retardation of the crystal growth.

References

1. El Hahab, M. I. JP Technol 1985, 1640.
2. Amjad, Z. J Colloid Interface Sci 1988, 123, 523.
3. Gabrielli, C.; Keddam, M.; Perrot, H.; Khalil, A.; Rosset, R; ZidDoune, M. J Appl Electrochem 1996, 26, 1125.
4. Troup D.H.; Richardson J. A. Werkstoffe Korrosion 1978, 29, 312.
5. Kazmlerczak, T. F.; Tomson M. B.; Nancollas, G. H. J Phys Chem 1982, 86, 103.
6. Salmone, J. C. Polymer Materials Encyclopedia; CRC Press: Boca Laton, FL, 1996.
7. Bardsley, J. H.; Robertson, S. T.; Schulman, J. E. Eur. Patent 04, 1992, 59, 661.
8. Misra, G. S.; Dubey, S. C. J Polymn Sci Poly Chem Ed. 1979, 17, 1373.
9. NACE Standard Test Method, TM0374–95.
10. Gabrielli, C.; Keddam, M.; Perrot, H.; Khalil, A.; Rosset, R.; Zidoune, M. J Appl Electrochem 1996, 26, 1125.
11. Simpson, L. J. Electrochem Acta 1998, 43, 2543.
12. Yan, J. F.; White, R. E.; Griffin, R. B. J Electrochem Soc 1993, 140, 1275.
13. Patel, S.; Nicol, A. J. Mater Perf 1996, 41.
14. Alice Arul Antony, Arul; Paruthimal Kalaignan, G.; Gopalan, A.; Balakrishnan, K.; Vasudevan, T.; Bull Electrochem 1999, 15, 124.
15. Silverstein, R. M.; Bassler G. C.; Terence, C. M. Spectrometric Identification of Organic Compounds; John Wiley & Sons: New York, 1961, 5th ed.
16. Dyer J. R. Application of Absorption Spectroscopy of Organic Compounds; Prentice-Hall of India Pvt Ltd: New Delhi, 1991; 8th ed.
17. Ledion, J.; Leory P.; Labbe, I. P. TSML Eau 1985.
18. Zidoune, M.; Khalil, A.; Sakyat, P.; Collin C.; Rossert, R. C A Acad Sci Paris 1992, 35; 1992, 795.
19. Deslouis, C.; Gabrielli, C.; Keddam, M.; Perrot, H.; Khalil, A.; Rossert, R.; Trobollet B.; Zidoune M. J Electrochem. Acta 1997, 42, 1219.
20. Deslouis, C.; Festy, D.; Gil, O.; Ruis, G.; Touzain, S.; Tribollet, B. J Electrochem Acta Vol. 43, 1998, 1891.
21. Sawada, K.; Ogino, T.; Suzuki, T. J Crystal Growth 1990, 106, 393.
22. Wada, N.; Yamashita, K.; Umegadi, T. J Crystal Growth 1995, 148, 297.
23. Austin, A. E.; Miller, J. F.; Vaughan, D. A.; Kircher, J. F. Desalination 1975, 16, 345.
24. Dalas, E.; Petros, G. K. Desalination 1990, 78, 403.
25. El Dahan, H. A.; Hegazy, H. S. Desalination 2000, 127, 111.
26. Imai, T.; Uchida, T.; Ano, S.; Tsuneki, T Mater Perf 1989, 41.